Precipitation Measurement at CESAR, the Netherlands

H. LEIJNSE,* R. UIJLENHOET, C. Z. VAN DE BEEK,+ AND A. OVEREEM

Hydrology and Quantitative Water Management Group, Wageningen University, Wageningen, Netherlands

T. OTTO, C. M. H. UNAL, Y. DUFOURNET, H. W. J. RUSSCHENBERG, AND J. FIGUERAS I VENTURA#

International Research Centre for Telecommunications and Radar, Delft University of Technology, Delft, Netherlands

H. KLEIN BALTINK AND I. HOLLEMAN@

Royal Netherlands Meteorological Institute, De Bilt, Netherlands

(Manuscript received and in final form 3 December 2009)

ABSTRACT

The Cabauw Experimental Site for Atmospheric Research (CESAR) observatory hosts a unique collection of instruments related to precipitation measurement. The data collected by these instruments are stored in a database that is freely accessible through a Web interface. The instruments present at the CESAR site include three disdrometers (two on the ground and one at 200 m above ground level), a dense network of rain gauges, three profiling radars (1.3, 3.3, and 35 GHz), and an X-band Doppler polarimetric scanning radar. In addition to these instruments, operational weather radar data from the nearby (~25 km) De Bilt C-band Doppler radar are also available. The richness of the datasets available is illustrated for a rainfall event, where the synergy of the different instruments provides insight into precipitation at multiple spatial and temporal scales. These datasets, which are freely available to the scientific community, can contribute greatly to our understanding of precipitation-related atmospheric and hydrologic processes.

1. Introduction

Precipitation is known to be highly variable over a range of scales in both space and time (e.g., Georgakakos et al. 1994; Fabry 1996; Uijlenhoet et al. 2003; Berne et al. 2004a,b; Ciach and Krajewski 2006). This has major implications for both our understanding of atmospheric processes (e.g., Trenberth 1998; Henzing et al. 2006) and the quality of remotely sensed precipitation (e.g., Gosset and Zawadzki 2001; Steiner et al. 2003; Gosset 2004; Miriovski et al. 2004; Leijnse et al. 2008, 2010). It is therefore very important to understand this space–time variability of precipitation at multiple scales.

In this paper, we describe the precipitation research that is conducted at the Cabauw Experimental Site for Atmospheric Research (CESAR) observatory. This site contains multiple sensors that measure precipitation at different scales in space and time. Datasets from several of these instruments span a number of years and are continuously growing. This combined dataset is unique in its length and the number of instruments it contains.

Upcoming satellite missions such as Global Precipitation Measurement (GPM; e.g., Rose and Chandrasekar 2005, 2006) and the Earth Clouds, Aerosols and Radiation Explorer (EarthCARE) (e.g., Battaglia and Simmer 2008; Koner et al. 2010), as well as existing space-based missions yielding precipitation data (such as derived from SEVIRI; see Roebeling and Holleman 2009), can greatly benefit from the precipitation measurements at the CESAR site. This is primarily achieved through validation, but the data collected at CESAR could also

* Current affiliation: Royal Netherlands Meteorological Institute, De Bilt, Netherlands.
+ Current affiliation: EARS, Delft, Netherlands.
# Current affiliation: Météo-France, Toulouse, France.
@ Current affiliation: Radboud University, Nijmegen, Netherlands.

Corresponding author address: Hidde Leijnse, Royal Netherlands Meteorological Institute, Wilhelminalaan 10, 3732 GK De Bilt, Netherlands.
E-mail: hidde.leijnse@knmi.nl

DOI: 10.1175/2010JHM1245.1

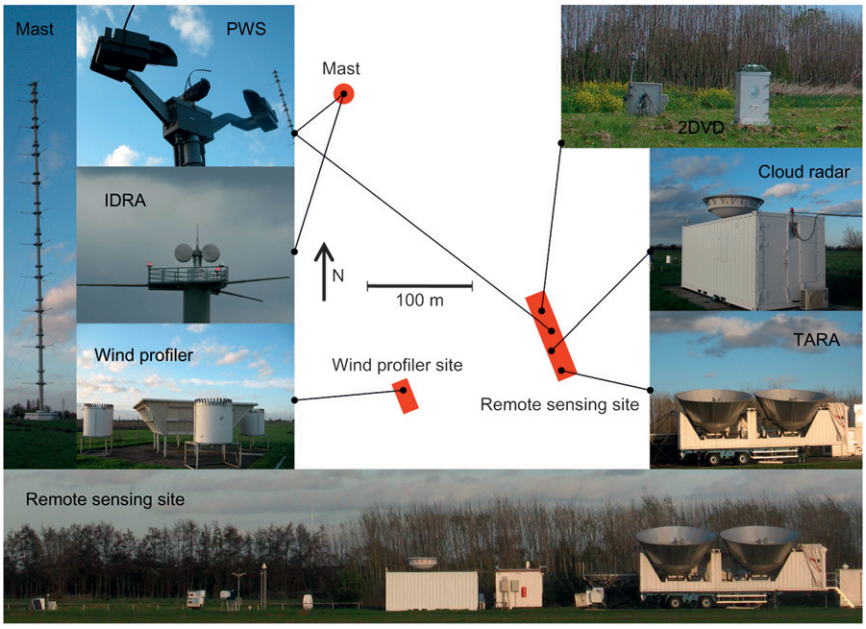

FIG. 1. Schematic drawing of the CESAR site layout, with locations and photographs of the different instruments discussed in this paper (photograph of IDRA is by Raymond Shaw and all others are by Hidde Leijnse).

contribute to improvement of retrieval algorithms. Numerical weather prediction (NWP) models rely heavily on proper representation of microphysics of clouds and precipitation. Again, datasets collected at CESAR can serve to validate and improve these representations (e.g., Lin and Colle 2009) but also as input to data assimilation schemes for NWP (e.g., Jung et al. 2008).

2. CESAR site description

CESAR is a consortium of three universities and five major research institutes (see online at http://www.cesar-observatory.nl). The CESAR site is located at 51.971°N, 4.927°E, between the villages of Cabauw and Lopik, the Netherlands, and is operated by the Royal Netherlands Meteorological Institute (KNMI).

The Netherlands has a temperate climate with prevailing westerly winds. Mean annual rainfall varies between 675 and 925 mm (800 mm at Cabauw), with little seasonal variation. Annual 24-h rainfall maxima generally occur from July to December, and annual 1-h rainfall maxima occur from June to September, mainly because of the larger influence of convective rainfall in the summer. Most precipitation in the Netherlands falls as rainfall, with occasional hail in summer thunderstorms. Some snow and hail events usually occur each winter. The precipitation systems that can be observed at the CESAR site range from stratiform to deep convection. For more details regarding the rainfall climatology of the Netherlands, see Schuurmans et al. (2007) and Overeem et al. (2008, 2009a,b).

The suite of instruments related to precipitation measurement at the CESAR site includes one scanning radar (9.5 GHz) and three profiling radars (1.3, 3, and 35 GHz), three disdrometers, and a dense network of rain gauges. The operational C-band weather radar network of the Netherlands also offers relatively high-resolution data, because one of the radars comprising this network is located at approximately 25 km from the CESAR site. In addition to these instruments, CESAR has multiple lidars and radiometers, an extensive radiation measurement site [Baseline Surface Radiation Network (BSRN); see, e.g., Wang et al. 2009], and a 213-m-high tower in which profiles of several variables such as temperature and wind are measured. Aerosols are sampled at 60 m in this mast, and turbulent fluxes are measured on the site as well. Hydrological data (ditch discharges, groundwater levels, and soil moisture) of the catchment around the CESAR site are also available (see Brauer et al. 2009). The availability of these other atmospheric and hydrological data means that precipitation can easily be linked to other atmospheric and hydrological processes. The CESAR site is a regular host to large measurement campaigns (see, e.g., Crewell et al. 2004; Su et al. 2009; Kulmala et al. 2009), which occasionally bring many additional instruments to the site. The instruments at the CESAR site are

TABLE 1. Specifications of the four radars at CESAR and the operational C-band weather radars. Note that the temporal resolution refers to the time for one scan for scanning radars (IDRA and the operational radars) and for one profile for profiling radars. The range (resolution, minimum, and maximum) and Doppler velocity v_D (resolution maximum) characteristics depend on the data acquisition mode for most radars. Maximum v_D values after dealiasing are listed in this table for IDRA, TARA, and the De Bilt C-band radar.

	IDRA	TARA	Cloud radar	Wind profiler	C-band radar
Radar type	FMCW	FMCW	pulsed	pulsed	pulsed
Polarization	dual polarization	dual polarization	selectable	N/A	horizontal
Frequency	9.475 GHz	3.3 GHz	35 GHz	1.29 GHz	5.6 GHz
Range resolution	3–30 m	3–75 m	89 m	60 m	0.5–1.0 km
Min range	230 m	200 m	250 m	150 m	N/A
Max range	<122 km	38 km	13 km	5.5 km	320 km
Max v_D	19 m s^{-1}	25 m s^{-1}	8.06 m s^{-1}	14.5 m s^{-1}	24 m s^{-1}
v_D resolution	0.03 m s^{-1}	0.03 m s^{-1}	0.126 m s^{-1}	0.23 m s^{-1}	0.189 m s^{-1}
Temporal resolution	1 min	1.5 s	15 s	5 min	5 min
Beamwidth	1.8°	2°	0.3°	6°	1°
Elevations	0.5°	0°–90°	90°	90°	0.3°–25°

concentrated at two locations, the remote sensing site and the tower, which are shown in Fig. 1, along with the locations of the precipitation-related instruments.

a. Radars

Two of the four radars at the CESAR site are operated by the Delft University of Technology (TU Delft): namely, the International Research Centre for Telecommunications and Radar (IRCTR) Drizzle Radar (IDRA; see Figueras i Ventura and Russchenberg 2009) and the Transportable Atmospheric Radar (TARA; see Heijnen et al. 2000). These two radars are both polarimetric frequency modulated continuous-wave (FMCW) radars with extremely high spatial resolutions. IDRA operates at X band, is located on top of the tower, and scans at 1 rpm at an elevation angle of 0.5°. Spectral polarimetry (Unal 2009) is applied in real-time data processing to suppress clutter and thus to enhance precipitation detection. TARA is a profiling radar that operates at S band, with beam azimuth and elevation that can be adjusted manually but remain fixed during operation. In the future, a raindrop-size-distribution retrieval algorithm will be devised that makes use of the joint measurements of TARA (through Doppler spectra; see Atlas et al. 1973) and IDRA (through polarimetric observables; see Seliga and Bringi 1976; Gorgucci et al. 2008).

KNMI operates a 35-GHz cloud radar (PDN100) and a 1290-MHz (Vaisala LAP-3000) wind profiler/radio acoustic sounding system (RASS) at the CESAR site. The cloud radar is a vertically pointing Doppler radar with a vertical resolution of 89 m and a temporal resolution of approximately 15 s. The wind profiler takes measurements in five different beam directions. In precipitation, the strength of the backscattered signal and the Doppler spectrum can be used to obtain information on the vertical distribution of precipitation and the associated drop size distributions.

The operational weather radar network of The Netherlands consists of two identical SELEX Meteor 360 AC C-band Doppler weather radars. Ground clutter correction and extension of the unambiguous velocity range (Sirmans et al. 1976; Holleman and Beekhuis 2003) are operationally applied to the data. The operational scanning of the KNMI weather radars generates a 14-elevation (0.3°, 0.4°, 0.8°, 1.1°, 2°, 3°, 4.5°, 6°, 8°, 10°, 12°, 15°, 20°, and 25°) volume. The 0.4° elevation is at approximately the height of IDRA at the location of the CESAR site (22.762-km range and 229.5° azimuth from the radar). For comparisons between the two, we will therefore use this elevation. The characteristics of the radars at the CESAR site and the operational C-band weather radars are given in Table 1.

b. In situ instruments

Three disdrometers are operated by Wageningen University at the CESAR site, one 2D video distrometer (2DVD; see Schönhuber et al. 1994; Kruger and Krajewski 2002) and two HSS present weather sensors (PWS; see Sheppard and Joe 2000). These disdrometers are optical disdrometers with measurement areas between 50 and 100 cm^2, which derive particle sizes and fall velocities from the known optical scattering properties of hydrometeors. The 2DVD and one PWS are located within 10 m of each other at the remote sensing site (see Fig. 1). The other PWS is located at 200-m altitude in the meteorological tower and can hence provide information on the particle size distribution aloft.

A dense network of approximately 15 tipping-bucket rain gauges is operated around the CESAR site by Wageningen University to investigate the short-range variability of rainfall (Schuurmans et al. 2007). The network has a radius of approximately 10 km, with a maximum distance between gauges of 15 km and one collocated

TABLE 2. Availability of data from different instruments. Products in the database include copolar horizontal reflectivity Z_{HH}, reflectivity Z, mean Doppler velocity v, Doppler velocity spread w, drop size distribution $N(D)$, optical extinction Q_{opt}, and rainfall intensity R. Note that operational C-band weather radar data are available through KNMI (additional IDRA data are available through http://data.3tu.nl/repository/resource:sensor-51970493-IDRA).

Instrument	Source	Start	Frequency	Products
IDRA	CDS	27 Jun 2008	5 min	Z_{HH}
TARA	CDS	campaigns only	variable	variable
Cloud radar	CDS	1 Aug 2001	15 s	Z, v, w
Wind profiler	CDS	1 Jan 1995	5 min	Z, v, w
C-band radar	KNMI	1 Feb 1998	5 min	Z, v, w
2DVD	CDS	1 Jul 2008	1 min	$N(D)$
PWS (3 m)	CDS	22 Feb 2006	1 min	$N(D)$, Q_{opt}
PWS (200 m)	CDS	20 Nov 2006	1 min	$N(D)$, Q_{opt}
Gauges	CDS	1 May 2004	10 min	R

gauge pair. The rain gauges have a volumetric resolution of 0.2 mm and are sampled at a temporal resolution of 0.5 s.

3. Data availability

To utilize the CESAR data to its full potential, it is important that users are able to freely access and retrieve the data in a user-friendly way with an acceptable response time and without any operator interference. KNMI has developed the CESAR database system (CDS) to address this need. The CDS has a Web-based portal through which data can be accessed (see online at http://www.cesar-database.nl).

The front end (Web portal) of the CDS comprises a self registration, a search function with a limited number of search options, and a download basket for ordering data files. Metadata on the dataset level is provided in the Web portal, as well as an option to preview the data by quick looks, which are stored with the data files in the database. The data are all stored in network common data form (netCDF) format (available online at http://www.unidata.ucar.edu/software/netcdf) and comply with the Climate and Forecast (CF) Metadata Convention version 1.4 (available online at http://cf-pcmdi.llnl.gov). The CDS has become operational in July 2009 and will be filled with many datasets from the operational continuous measurement program, measurements executed by visiting researchers, and datasets from (inter)national campaigns hosted at CESAR (e.g., Crewell et al. 2004; Su et al. 2009; Kulmala et al. 2009).

Most data from the instruments presented in section 2 are or will become available through this database.

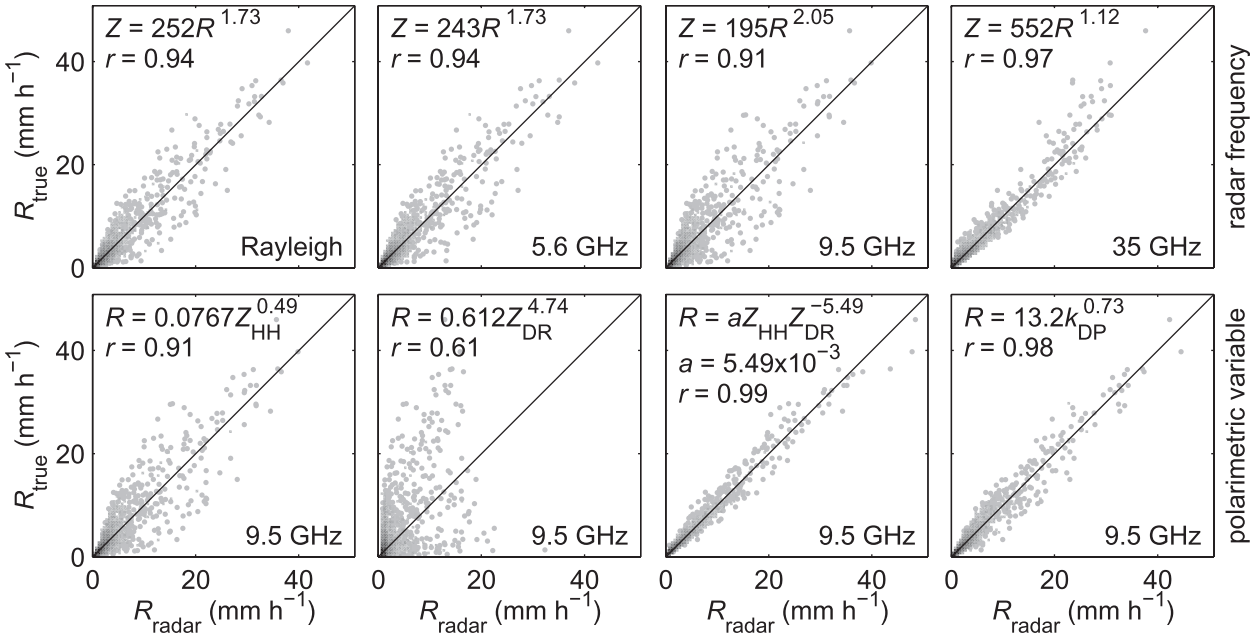

FIG. 2. Results of fits of power-law relations between rainfall intensity on the one hand and radar variables on the other based on 9 months (March–November 2009) of 2DVD data. The graphs show rainfall intensities estimated from radar variables (R_{radar}) on the x axes, and true rainfall intensities (R_{true}) on the y axes, with the corresponding correlation coefficient between the two (r) given. The density of points in these graphs is indicated by the darkness of the shading (individual points are plotted in areas with low point density). Shown are (top) the results for radar variables computed using scattering matrices for different radar wavelengths (corresponding to the radar frequencies employed at the CESAR site) and using the Rayleigh scattering approximation with spherical raindrops and (bottom) results for polarimetric X-band radar (e.g., IDRA), where rainfall is retrieved from different polarimetric variables. Note that the third panel in (top) is the same as first panel in (bottom).

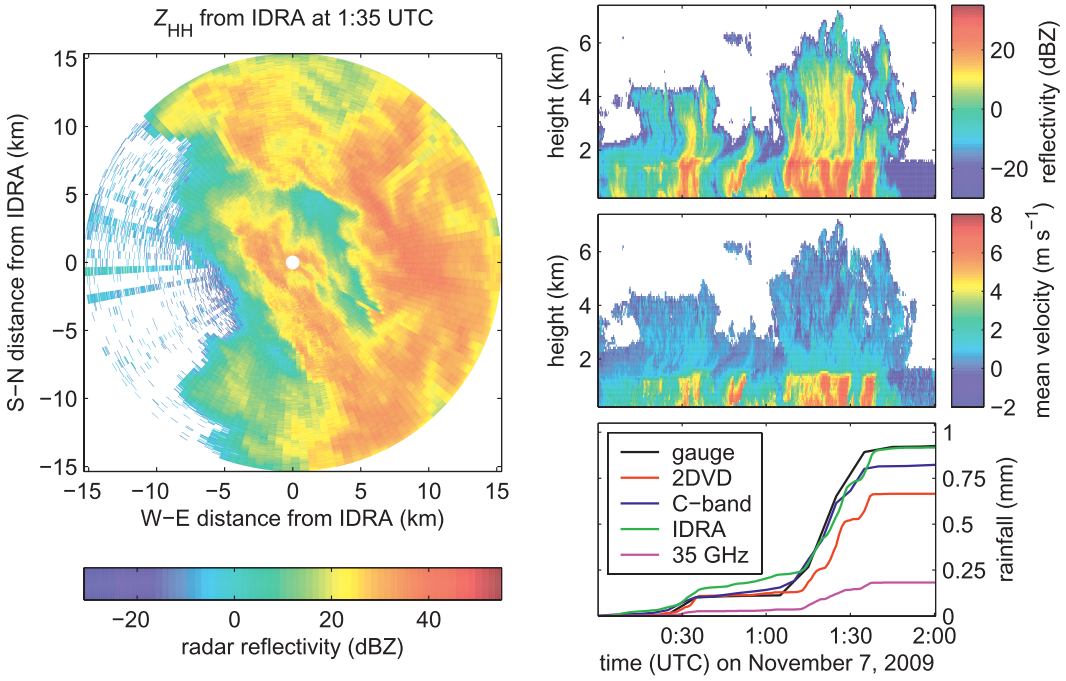

FIG. 3. Several aspects of the rainfall event on 7 Nov 2009: (left) radar reflectivities measured by IDRA at 0135 UTC and (right) time series of (top) reflectivity and (middle) mean Doppler velocity as a function of height as measured by the 35-GHz cloud radar for the event. (bottom right) Also shown is the time evolution of rainfall accumulation for this event measured by a rain gauge, the 2DVD, the operational C-band radar located in De Bilt, IDRA, and the lowest range cell (250 m) of the 35-GHz cloud radar.

Operational C-band radar data are stored in hierarchical data format 5 (HDF5; available online at http://hdfgroup.org/HDF5). Table 2 lists details regarding data availability for the different instruments discussed in section 2.

4. Examples

Nine months of 2DVD data have been employed to derive power-law radar rainfall retrieval relations. The results of these power-law fits are shown in Fig. 2, where retrieved rainfall intensities are compared to true values of R. Radar variables have been computed using the Rayleigh approximation with spherical raindrops (top-left panel) and using T-matrix scattering computations (Mishchenko 2000) with raindrop oblateness ratios according to Andsager et al. (1999; all other panels). These analyses have been carried out for different radar frequencies (corresponding to radar frequencies employed at CESAR; top panels) and for different X-band polarimetric variables. It is clear from Fig. 2 that using polarimetric retrieval relations (particularly Z_{HH}/Z_{DR} and K_{DP}) may greatly reduce scatter resulting from DSD variability.

Figure 3 shows an overview of a rainfall event that occurred on 7 November 2009. The vertical profiles of reflectivity and mean Doppler velocity measured by the 35-GHz cloud radar clearly show the presence of a melting layer at ~1.5 km, which means that both the 0.4° elevation of the operational C-band radar and IDRA are measuring liquid precipitation. The plan position indicator (PPI) of reflectivities from IDRA (including a calibration correction based on comparison with 2DVD-derived reflectivities; this calibration offset has been confirmed by Otto and Russchenberg (2010)) shows the very fine spatial structure that is present in this event, indicating the great potential of this extremely high-resolution radar for studying this structure. Time series of rainfall accumulations measured by different instruments (relations from Fig. 2 are used for radar rainfall estimates) are shown in Fig. 3 (bottom right) to be similar. Appropriate areal averages of rainfall intensities have been used for the C-band radar and IDRA to compensate for storm cell advection between radar scans (see Fabry et al. 1994). The underestimation by the lowest range cell (250 m) of the 35-GHz cloud radar is likely due to attenuation resulting from wetting of the material covering the antenna.

Figure 4 shows a comparison of PPIs from IDRA and the operational C-band radar. For this purpose, IDRA data have been averaged so that they fit on the C-band radar grid. Comparing Figs. 3 and 4 again shows the extremely detailed information on the spatial structure that can be obtained using IDRA. The two PPIs look

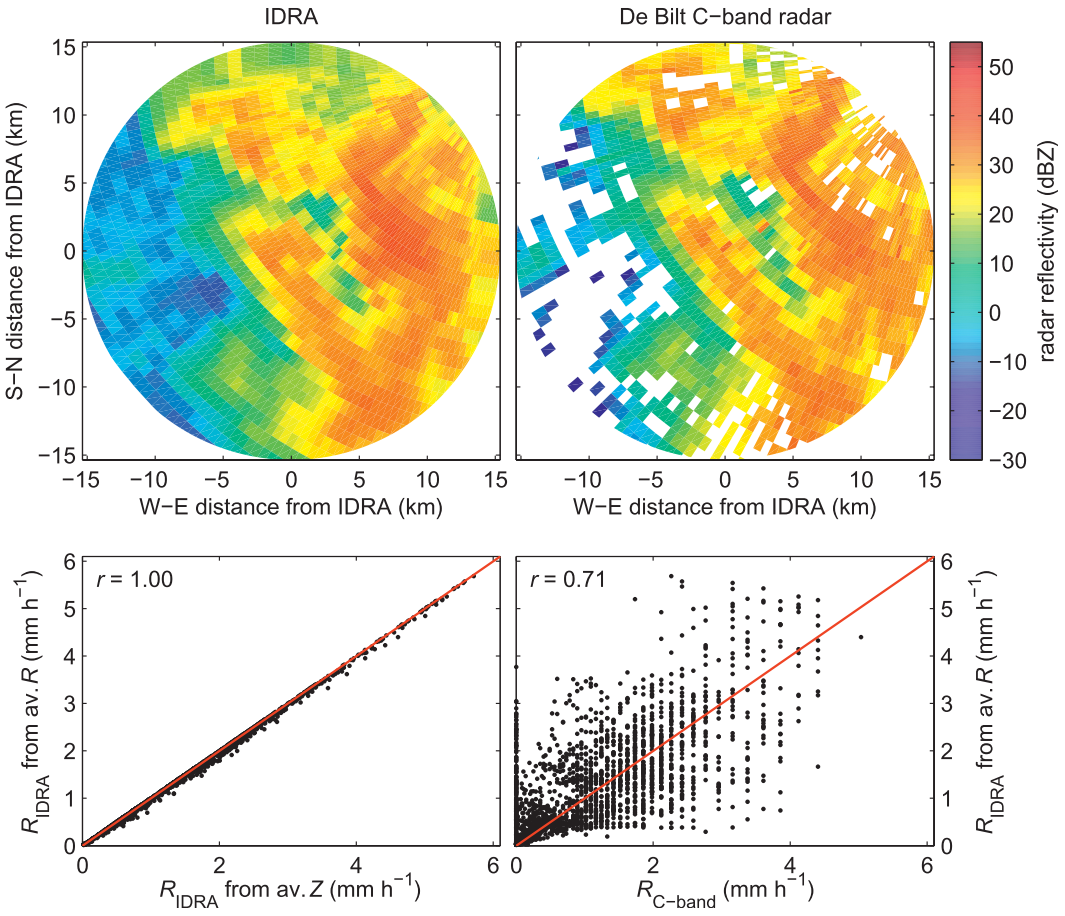

FIG. 4. (top) Comparison of PPIs (dBZ) from the IDRA X-band and De Bilt C-band radars at 0135 UTC 7 Nov 2009. IDRA reflectivities have been averaged for each C-band radar pixel, taking the beam shape of this radar into account. Only the De Bilt C-band radar data that are within the IDRA range are shown for ease of comparison. (bottom) Shown are a comparison of rainfall intensities estimated by averaging rainfall intensities computed on the original IDRA grid on the one hand (y axes) and rainfall intensities computed from (left) averaged IDRA reflectivities and (right) operational C-band radar reflectivities on the other. Correlation coefficients r are given in these graphs.

quite similar. However, when quantitatively comparing rainfall intensities for each grid point in the top panels (Fig. 4, bottom right), there is a considerable amount of scatter. This could have been partially caused by the fact that a nonlinear retrieval relation is used in combination with subgrid rainfall variability. However, the bottom-left panel of Fig. 4 shows that this is not the case here.

5. Conclusions and perspectives

In this paper, the potential for precipitation science at the Cabauw Experimental Site for Atmospheric Research (CESAR) observatory has been illustrated. The unique combination of instruments, both in situ and remote sensing, provides data to quantitatively study many processes related to precipitation, on a wide range of spatial and temporal scales. The individual datasets collected by each of these instruments already have great value. However, it is the synergetic use of these instruments that provides the greatest potential for improving our understanding of atmospheric and hydrologic processes related to precipitation. One important aspect is related to the space–time variation of the microstructure of precipitation. The polarimetric variables measured by IDRA (e.g., Seliga and Bringi 1976; Gorgucci et al. 2008), vertically pointing Doppler radar (e.g., Hauser and Amayenc 1981, 1983; Kollias et al. 2002), and a combination thereof (Unal and Moisseev 2004; Moisseev et al. 2006; Spek et al. 2008; Unal 2009) can be used to obtain information on the microphysics of precipitation with unprecedented extent and resolution.

A recently developed dedicated database provides free and easy Web access to the data collected at the CESAR site. This database and Web portal allow many

scientists to work with this unique dataset. It is expected that this database will contribute greatly to our understanding of precipitation-related atmospheric and hydrologic processes. In our view, sharing data among scientists, such as is common practice in the United States, is a development that should be greatly encouraged, because it can lead to a more open scientific debate and ultimately lead to a better and more complete understanding of physical processes. The CESAR consortium, through its database, aims to contribute to this development.

Acknowledgments. We thank Jacques Warmer (KNMI) for the aid with most of the instruments presented in this paper. H. Leijnse was financially supported by the Netherlands Organisation for Scientific Research through a grant in the framework of the Water Programme.

REFERENCES

Andsager, K., K. V. Beard, and N. F. Laird, 1999: Laboratory measurements of axis ratios for large raindrops. *J. Atmos. Sci.,* **56,** 2673–2683.

Atlas, D., R. C. Srivasta, and R. S. Sekhon, 1973: Doppler radar characteristics of precipitation at vertical incidence. *Rev. Geophys.,* **11,** 1–35.

Battaglia, A., and C. Simmer, 2008: How does multiple scattering affect the spaceborne W-band radar measurements at ranges close to and crossing the sea-surface range? *IEEE Trans. Geosci. Remote Sens.,* **46,** 1644–1651.

Berne, A., G. Delrieu, H. Andrieu, and J.-D. Creutin, 2004a: Influence of the vertical profile of reflectivity on radar-estimated rain rates at short time steps. *J. Hydrometeor.,* **5,** 296–310.

——, ——, J.-D. Creutin, and C. Obled, 2004b: Temporal and spatial resolution of rainfall measurements required for urban hydrology. *J. Hydrol.,* **299,** 166–179.

Brauer, C. C., J. N. M. Stricker, and R. Uijlenhoet, 2009: Linking meteorology and hydrology: measuring water balance terms in Cabauw, the Netherlands. *Proc. Eighth Int. Symp. Tropospheric Profiling,* Delft, Netherlands, RIVM, KNMI, and TU-Delft, S12–P01.

Ciach, G. J., and W. F. Krajewski, 2006: Analysis and modelling of spatial correlation structure in small-scale rainfall in central Oklahoma. *Adv. Water Resour.,* **29,** 1450–1463, doi:10.1016/j.advwatres.2005.11.003.

Crewell, S., and Coauthors, 2004: The BALTEX BRIDGE Campaign: An integrated approach for a better understanding of clouds. *Bull. Amer. Meteor. Soc.,* **85,** 1565–1584.

Fabry, F., 1996: On the determination of scale ranges for precipitation fields. *J. Geophys. Res.,* **101** (D8), 12 819–12 826.

——, A. Bellon, M. R. Duncan, and G. L. Austin, 1994: High resolution rainfall measurements by radar for very small basins: The sampling problem reexamined. *J. Hydrol.,* **161,** 415–428.

Figueras i Ventura, J., and H. W. J. Russchenberg, 2009: Towards a better understanding of the impact of anthropogenic aerosols in the hydrological cycle: IDRA, IRCTR drizzle radar. *Phys. Chem. Earth,* **34,** 88–92, doi:10.1016/j.pce.2008.02.038.

Georgakakos, K. P., A. A. Carsteanu, P. L. Sturdevant, and J. A. Cramer, 1994: Observation and analysis of Midwestern rain rates. *J. Appl. Meteor.,* **33,** 1433–1444.

Gorgucci, E., V. Chandrasekar, and L. Baldini, 2008: Microphysical retrievals from dual-polarization radar measurements at X band. *J. Atmos. Oceanic Technol.,* **25,** 729–741.

Gosset, M., 2004: Effect of nonuniform beam filling on the propagation of the radar signal at X-band frequencies. Part II: Examination of differential phase shift. *J. Atmos. Oceanic Technol.,* **21,** 358–367.

——, and I. Zawadzki, 2001: Effect of nonuniform beam filling on the propagation of the radar signal at X-band frequencies. Part I: Changes in the $k(Z)$ relationship. *J. Atmos. Oceanic Technol.,* **18,** 1113–1126.

Hauser, A., and P. Amayenc, 1981: A new method for deducing hydrometeor-size distributions and vertical air motions from Doppler radar measurements at vertical incidence. *J. Appl. Meteor.,* **20,** 547–555.

——, and ——, 1983: Exponential size distributions of raindrops and vertical air motions deduced from vertically pointing Doppler radar data using a new method. *J. Appl. Meteor.,* **22,** 407–418.

Heijnen, S. H., L. P. Ligthart, and H. W. J. Russchenberg, 2000: First measurements with TARA: An S-band transportable atmospheric radar. *Phys. Chem. Earth,* **25,** 995–998.

Henzing, J. S., D. J. L. Olivie, and P. F. J. van Velthoven, 2006: A parameterization of size resolved below cloud scavenging of aerosols by rain. *Atmos. Chem. Phys.,* **6,** 3363–3375.

Holleman, I., and H. Beekhuis, 2003: Analysis and correction of dual PRF velocity data. *J. Atmos. Oceanic Technol.,* **20,** 443–453.

Jung, Y., G. Zhang, and M. Xue, 2008: Assimilation of simulated polarimetric radar data for a convective storm using the ensemble Kalman filter. Part I: Observation operators for reflectivity and polarimetric variables. *Mon. Wea. Rev.,* **136,** 2228–2245.

Kollias, P., B. A. Albrecht, and F. Marks Jr., 2002: Why Mie? *Bull. Amer. Meteor. Soc.,* **83,** 1471–1483.

Koner, P. K., A. Battaglia, and C. Simmer, 2010: A rain-rate retrieval algorithm for attenuated radar measurements. *J. Appl. Meteor. Climatol.,* **49,** 381–393.

Kruger, A., and W. F. Krajewski, 2002: Two-dimensional video disdrometer: A description. *J. Atmos. Oceanic Technol.,* **19,** 602–617.

Kulmala, M., and Coauthors, 2009: Introduction: European Integrated Project on Aerosol Cloud Climate and Air Quality interactions (EUCAARI)—Integrating aerosol research from nano to global scales. *Atmos. Chem. Phys.,* **9,** 2825–2841.

Leijnse, H., R. Uijlenhoet, and J. N. M. Stricker, 2008: Microwave link rainfall estimation: Effects of link length and frequency, temporal sampling, power resolution, and wet antenna attenuation. *Adv. Water Resour.,* **31,** 1481–1493, doi:10.1016/j.advwatres.2008.03.004.

——, ——, and A. Berne, 2010: Errors and uncertainties in microwave link rainfall estimation explored using drop size measurements and high-resolution radar data. *J. Hydrometeor.,* **11,** 1330–1344.

Lin, Y., and B. A. Colle, 2009: The December 2001 IMPROVE-2 event: Observed microphysics and comparisons with the weather research and forecasting model. *Mon. Wea. Rev.,* **137,** 1372–1392.

Miriovski, B. J., and Coauthors, 2004: An experimental study of small-scale variability of radar reflectivity using disdrometer observations. *J. Appl. Meteor.,* **43,** 106–118.

Mishchenko, M. I., 2000: Calculation of the amplitude matrix for a nonspherical particle in a fixed orientation. *Appl. Opt.,* **39,** 1026–1031.

Moisseev, D. N., V. Chandrasekar, C. M. H. Unal, and H. W. J. Russchenberg, 2006: Dual-polarization spectral analysis for retrieval of effective raindrop shapes. *J. Atmos. Oceanic Technol.,* **23,** 1682–1695.

Otto, T., and H. W. J. Russchenberg, 2010: Estimation of the raindrop-size distribution at X-band using specific differential phase and differential backscatter phase. *Proc. Sixth European Conf. on Radar in Meteorology and Hydrology: Adv. in Radar Technology,* Sibiu, Romania, ERAD, 171–176.

Overeem, A., A. Buishand, and I. Holleman, 2008: Rainfall depth-duration-frequency curves and their uncertainties. *J. Hydrol.,* **348,** 124–134, doi:10.1016/j.jhydrol.2007.09.044.

——, ——, and ——, 2009a: Extreme rainfall analysis and estimation of depth-duration-frequency curves using weather radar. *Water Resour. Res.,* **45,** W10424, doi:10.1029/2009WR007869.

——, I. Holleman, and A. Buishand, 2009b: Derivation of a 10-year radar-based climatology of rainfall. *J. Appl. Meteor. Climatol.,* **48,** 1448–1463.

Roebeling, R. A., and I. Holleman, 2009: SEVIRI rainfall retrieval and validation using weather radar observations. *J. Geophys. Res.,* **114,** D21202, doi:10.1029/2009JD012102.

Rose, C. R., and V. Chandrasekar, 2005: A systems approach to GPM dual-frequency retrieval. *IEEE Trans. Geosci. Remote Sens.,* **43,** 1816–1826.

——, and ——, 2006: A GPM dual-frequency retrieval algorithm: DSD profile-optimization method. *J. Atmos. Oceanic Technol.,* **23,** 1372–1383.

Schönhuber, M., H. Urban, J. P. V. Poiares Baptista, W. L. Randeu, and W. Riedler, 1994: Measurements of precipitation characteristics by a new disdrometer. *Proc. Atmospheric Physics and Dynamics in the Analysis and Prognosis of Precipitation Fields,* Rome, Italy.

Schuurmans, J. M., M. F. P. Bierkens, E. J. Pebesma, and R. Uijlenhoet, 2007: Automatic prediction of high resolution daily rainfall fields for multiple extents: The potential of operational radar. *J. Hydrometeor.,* **8,** 1204–1224.

Seliga, T. A., and V. N. Bringi, 1976: Potential use of radar differential reflectivity measurements at orthogonal polarizations for measuring precipitation. *J. Appl. Meteor.,* **15,** 69–76.

Sheppard, B. E., and P. I. Joe, 2000: Automated precipitation detection and typing in winter: A two-year study. *J. Atmos. Oceanic Technol.,* **17,** 1493–1507.

Sirmans, D., D. Zrnic, and B. Baumgarner, 1976: Extension of maximum, unambiguous Doppler velocity by use of 2 sampling rates. *Bull. Amer. Meteor. Soc.,* **57,** 856.

Spek, A. L. J., C. M. H. Unal, D. N. Moisseev, H. W. J. Russchenberg, V. Chandrasekar, and Y. Dufournet, 2008: A new technique to categorize and retrieve the microphysical properties of ice particles above the melting layer using radar dual-polarization spectral analysis. *J. Atmos. Oceanic Technol.,* **25,** 482–497.

Steiner, M., T. L. Bell, Y. Zhang, and E. F. Wood, 2003: Comparison of two methods for estimating the sampling-related uncertainty of satellite rainfall averages based on a large radar dataset. *J. Climate,* **16,** 3759–3778.

Su, Z., and Coauthors, 2009: EAGLE 2006—Multi-purpose, multi-angle and multi-sensor in-situ and airborne campaigns over grassland and forest. *Hydrol. Earth Syst. Sci.,* **13,** 833–845.

Trenberth, K. E., 1998: Atmospheric moisture residence times and cycling: Implications for rainfall rates and climate change. *Climatic Change,* **39,** 667–694.

Uijlenhoet, R., M. Steiner, and J. A. Smith, 2003: Variability of raindrop size distributions in a squall line and implications for radar rainfall estimation. *J. Hydrometeor.,* **4,** 43–61.

Unal, C. M. H., 2009: Spectral polarimetric radar clutter suppression to enhance atmospheric echoes. *J. Atmos. Oceanic Technol.,* **26,** 1781–1797.

——, and D. N. Moisseev, 2004: Combined Doppler and polarimetric radar measurements: Correction for spectrum aliasing and nonsimultaneous polarimetric measurements. *J. Atmos. Oceanic Technol.,* **21,** 443–456.

Wang, P., W. H. Knap, P. K. Munneke, and P. Stammes, 2009: Clear-sky shortwave radiative closure for the Cabauw Baseline Surface Radiation Network site, Netherlands. *J. Geophys. Res.,* **114,** D14206, doi:10.1029/2009JD011978.